JOURNAL OF SOLID STATE CHEMISTRY 29, 323–337 (1979)

In Situ Studies of Electrode Reactions: The Mechanism of Lithium Intercalation in TiS_2*

R. R. CHIANELLI,† J. C. SCANLON, AND B. M. L. RAO

Corporate Research Laboratories, Exxon Research and Engineering Company, Linden, New Jersey 07036

Received November 3, 1978

The mechanism of lithium intercalation into TiS_2 is poorly understood even though the system Li_xTiS_2 ($0 \leq x \leq 1$) has been extensively studied. This mechanism is critical in the functioning of Li/TiS_2 nonaqueous batteries. In this report we describe several techniques which are used to study this mechanism. These methods consist of *ex situ* and *in situ* optical and X-ray techniques which yield information regarding the mechanism of lithium intercalation and factors which effect this process during the operation of Li/TiS_2 batteries.

The ternary phase Li_xTiS_2 ($0 \leq x \leq 1$) has been the subject of intense study because of its superior performance as the active cathode material in a reversible lithium nonaqueous battery system (*1–3*). The reversibility of the TiS_2 cathodes arises in part from the unusual morphological nature of the intercalation reaction in which the lithium atoms slip into the van der Waals gap between the TiS_2 layers (Fig. 1). This process occurs at the cathode during discharge from $x = 0$ (TiS_2 fully charged) until $x = 1$ ($LiTiS_2$ fully discharged) with intermediate values of x in Li_xTiS_2 occurring in between. Upon recharge the reverse process occurs with reformation of the fully charged TiS_2. During charge and discharge no chemical bonds are broken and the TiS_2 layers remain intact. This type of reaction, in which structural integrity is retained, has been termed a topochemical reaction (of which the intercalation reaction is a special case) and the importance of topochemistry in determining cathode reversibility has been discussed (4).

Although the solid state chemistry and physics of the Li_xTiS_2 system has been studied in detail (*5–9*), the mechanism of lithium intercalation into TiS_2 is not fully understood. This mechanism probably involves several steps: absorption of a lithium atom at the TiS_2 surface, giving up by the lithium atom of an electron to the TiS_2 layers, opening of the layers, and diffusion of the Li atoms into the crystal. In this paper we describe the results of several techniques used to study the intercalation mechanism.

Optical *ex situ* Studies

For this study we have chosen the reaction of *n*-butyllithium with di- and trichalcogenides which has recently been reported (*5, 10*). This reaction has been shown to be related to electrochemical lithiation and has been termed "electrodeless

* Paper presented at the 1978 Americal Chemical Society Annual Meeting, "Symposium on Solid State Chemistry of Batteries, Electrodes, and Electrolytes, September 13, 1978, Miami, Florida."

† To whom correspondence should be sent.

0022-4596/79/090323-17$02.00/0

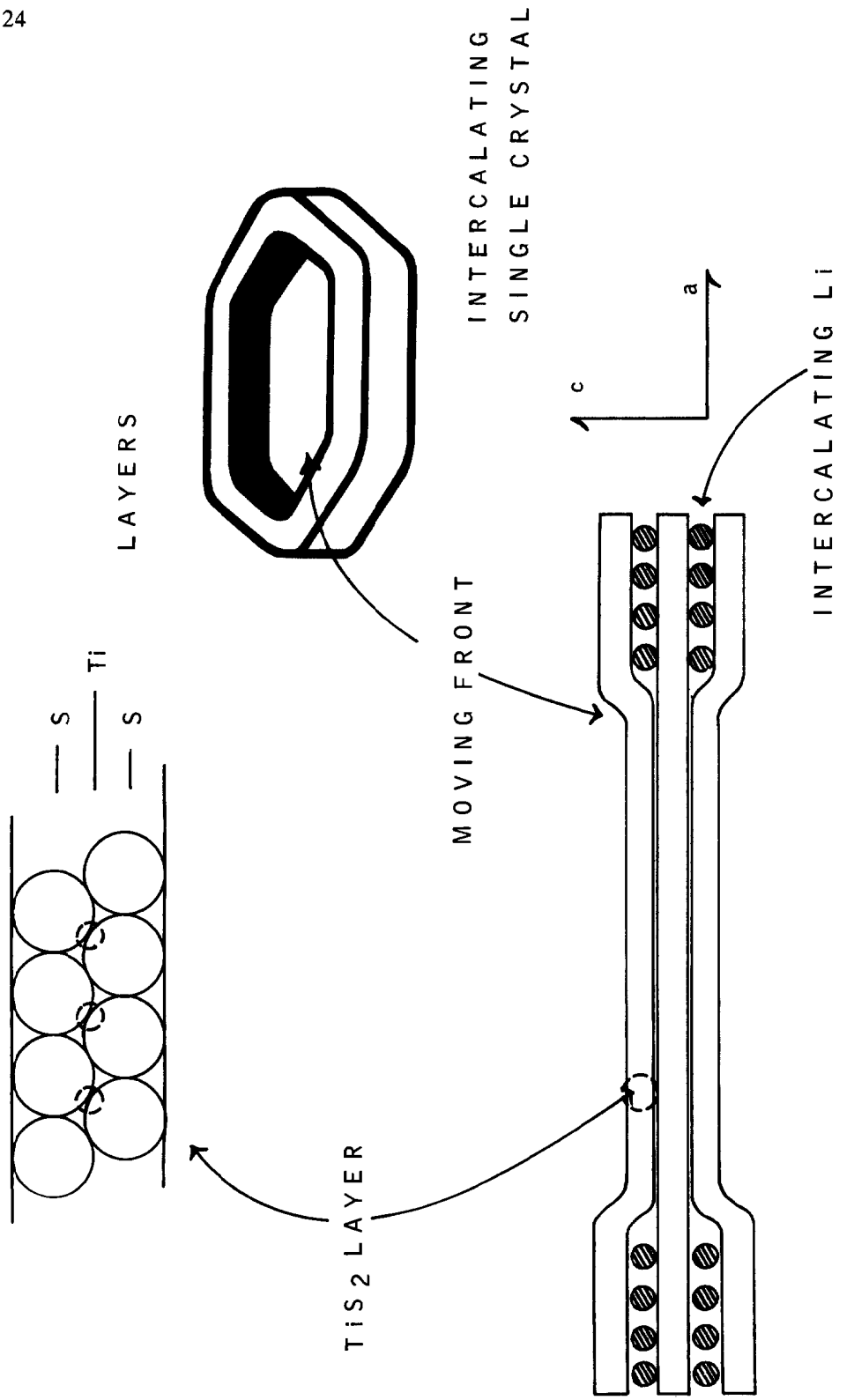

FIG. 1. Lithium intercalation in TiS_2.

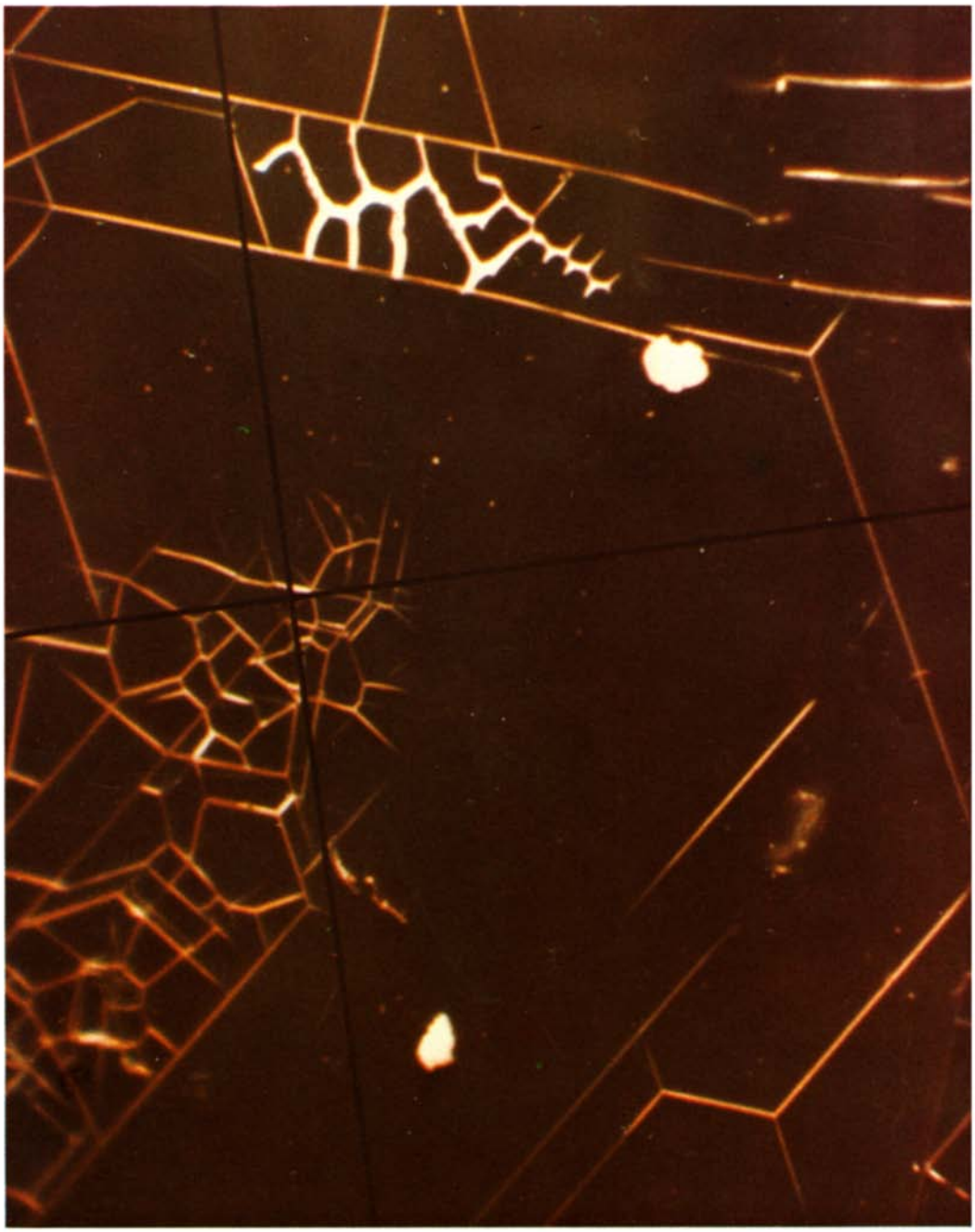

FIG. 2. Cracking in TiS_2 crystal; 45° illumination. Magnification approximately 250×. One inch is approximately 100 μm.

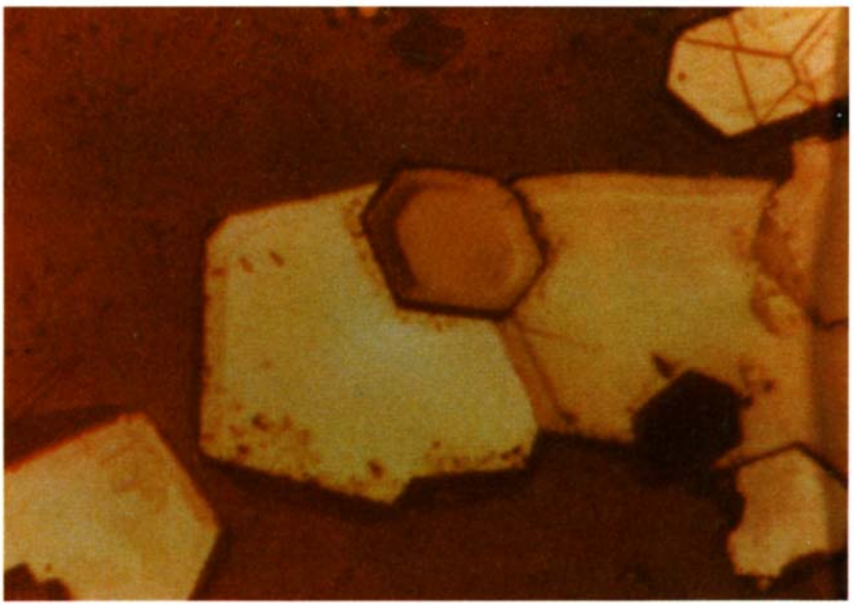

FIG. 5. Lithiation of perfect TiS_2 crystal, showing front between Li_xTiS_2 and TiS_2.

lithiation" (*11*). The *n*-butyllithium reacts with the TiS_2 to give $LiTiS_2$:

$$TiS_2 + CH_3(CH_2)_3\text{–}Li \rightarrow LiTiS_2 + \tfrac{1}{2}CH_3(CH_2)_6CH_3$$

The reactant (*n*-butyllithium) and the product (octane) are optically transparent, allowing clear observation of the intercalation of single crystals of TiS_2. A selection of crystals varying in size from about 0.01 to 1 mm were placed in suitable cells and the reaction was followed with time as described in Ref. (*12*).

During the intercalation of TiS_2 with Li from *n*-butyllithium, three distinct effects were seen.

(*i*) *Initial coloration.* During early stages of intercalation, small crystallites of TiS_2 on the surface of larger crystals were seen to turn brown when viewed against the gold-yellow of TiS_2 in incident illumination. This we interpret as a bending or displacement of the TiS_2 layers out of the plane of incidence of the optical axis of illumination, causing the layers to become nonreflective. This bending is in turn caused by Li lifting the edges of the crystallites as they diffuse into the unintercalated regions. This coloration disappears as the surface crystallites become fully intercalated and return to their position perpendicular to the incident light beam.

(*ii*) *Cracking of large TiS_2 crystallites.* Most crystallites showed an increasing amount of cracking and rifting as the reaction proceeded. The initial coloration often disappeared when cracks appeared, indicating that the strain of bending the layers was relieved upon cracking. The cracking usually occurred along geometrically significant angles (60°, 120°, or 90°) as indicated in Fig. 2. The cracks were usually less than 5 μm wide but in many cases deep rifts occurred greater than 10 μm wide. Closer examination of these rifts showed that they were V-shaped in cross section and steps could be seen along the walls of the cracks (Fig. 3). SEM photographs showed that these cracks extended deeply into the crystal (Fig. 4). We believe that the crystals cracked along imperfections due to "twinning" or stack faults which occur in TiS_2 (*13*).

(*iii*) *Behavior of small perfect crystals.* The cracking described above did not extend to areas below about 10 μm and the crystal as a whole retained its crystalline integrity as determined by X rays. Most larger crystals and crystals with imperfections showed this effect. Smaller crystals with perfect hexagonal morphology (less than 0.1 mm) showed the effect indicated in Fig. 5. A front beginning at the edge of the crystal moved through the crystal, until it disappeared at the center 4 to 5 hr later for an average crystal of about 50 μm. Crystals which showed this effect were not cracked after intercalation was complete. A lattice expansion of approximately 10% occurs upon intercalation with lithium, and the front shown in the hexagonal crystallite (Fig. 5) is the boundary between the expanded and unexpanded lattice (also shown schematically in Fig. 6). The front is quite sharp initially but becomes broader as the center of the crystal is reached. Generally, the boundary between the TiS_2 and $LiTiS_2$ portions of the crystal was about 2 μm. X-Ray studies of the *n*-butyllithation of TiS_2 with time showed the presence of 001 reflections of intercalated and unintercalated material with no smearing between them, in agreement with the optical study.

The width of the transition zone was found to be 2 ± 1 μm in all cases. Thus, large crystals (50 μm) as shown in Fig. 5 appear to have fairly sharp boundary areas whereas smaller crystals (5.6 μm) have sloping less-well-defined fronts. The estimation of the boundary width depended to a certain degree on the observation techniques used and could not be determined to better than ±1 μm for the larger crystals. For smaller crystals the transition zone from $LiTiS_2$ to TiS_2 was approximately 50% of the total width of the crystal and thus the front position was less

FIG. 3. Cracking of Li_xTiS_2, showing deep rifts.

easily determined. The movement of this front through the crystal gives a measurement of the rate of intercalation. If we approximate the hexagonal crystal by a cylindrical crystal of radius r_0 a calculation shows that the total flux ($J = g/cm^2 \cdot sec$) across a unit edge area of the crystals as a function of time (t) is given by: $r = (2J/\rho)t$, where ρ is the density of the crystal. If the flux is constant a plot of r (where r is now the

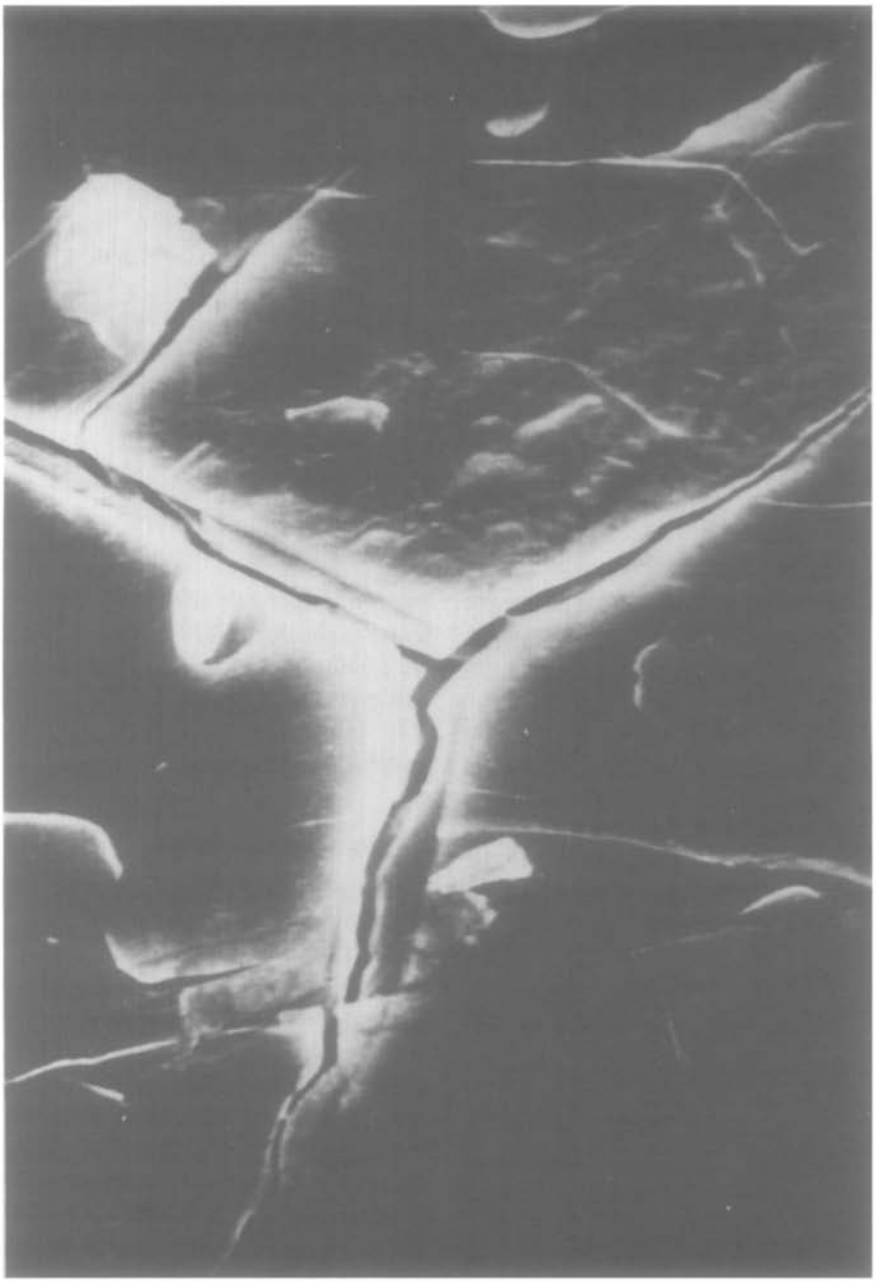

FIG. 4. Cracking of crystals upon lithiation; SEM. One inch is approximately 10 μm.

radius of the front moving through the crystal) will give a straight line with slope J. This was true for two crystals of $r_0 = 40$ μm and $r_0 = 5.6$ μm as shown in Figs. 7 and 8. However, the flux in the larger crystal (1.3×10^{-8}) is significantly slower than in the smaller crystal (18×10^{-8}). Although part of this effect may be related to the greater uncertainty in measuring the position of the front in the smaller crystal, we believe that

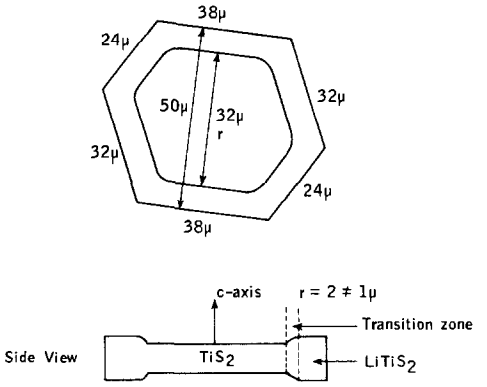

FIG. 6. Schematic lithiating 50-μm crystal, showing transition zone.

this is due primarily to the thickness of the crystal. The 5.6-μm crystal was much thinner than the 40-μm crystal as roughly determined by the focusing of the microscope on the glass slide and the top of the crystallite. We can see by referring to Fig. 6 that the strain induced during intercalation of thick crystal would be much greater than that induced in a thin crystal. Because the layers must flex considerably during the process, diffusion in thicker crystals may be retarded by the layers binding up. The effect could be confirmed by accurate observation of crystals of different thickness and size. Such an

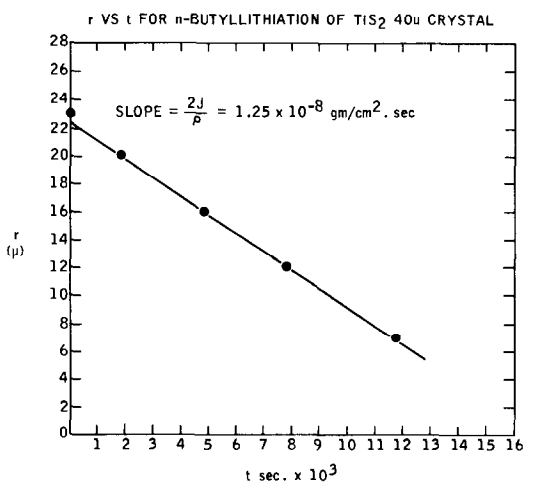

FIG. 7. Position of front vs time for 40-μm TiS_2 crystal ($J = 1.25 \times 10^{-8}$ g/cm^2 · sec).

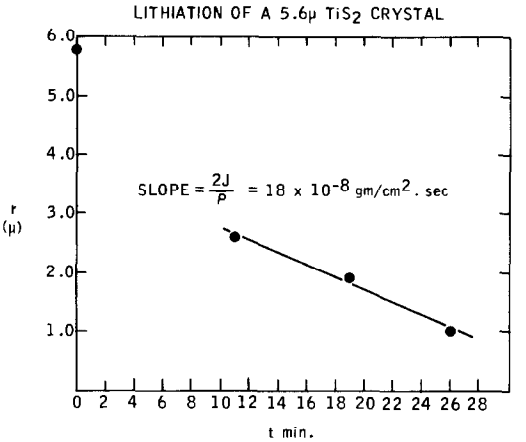

FIG. 8. Position of front vs time for 5.6-μm TiS_2 crystal ($J = 18 \times 10^{-8}$ g/cm^2 · sec).

experiment would also yield basic information on the flexibility of individual layers as related to basic bonding properties within the layers. In fact, we have shown that very thin layers (~40 Å) of these compounds exhibit remarkable flexibility (*14*).

In Situ Optical Studies

The previously described optical studies of the lithium intercalation of TiS_2 from *n*-butyllithium suffer the disadvantage that the process is irreversible and thus of limited use in generating information regarding effects which govern the reversible intercalation and deintercalation which occur in operating batteries. Such effects may be faster rates of intercalation after the initial intercalation rates as a function of cycles (repeated intercalation and deintercalation). In this section we describe a technique used for optical studies of an electrochemical cell with the possibility of lithium intercalation in TiS_2 (discharge process) and lithium deintercalation from TiS_2 (charge process). A cell which allows simultaneous or individual observation of the cathode or anode is shown schematically in Fig. 9. The cathode was a single crystal of TiS_2 which had been

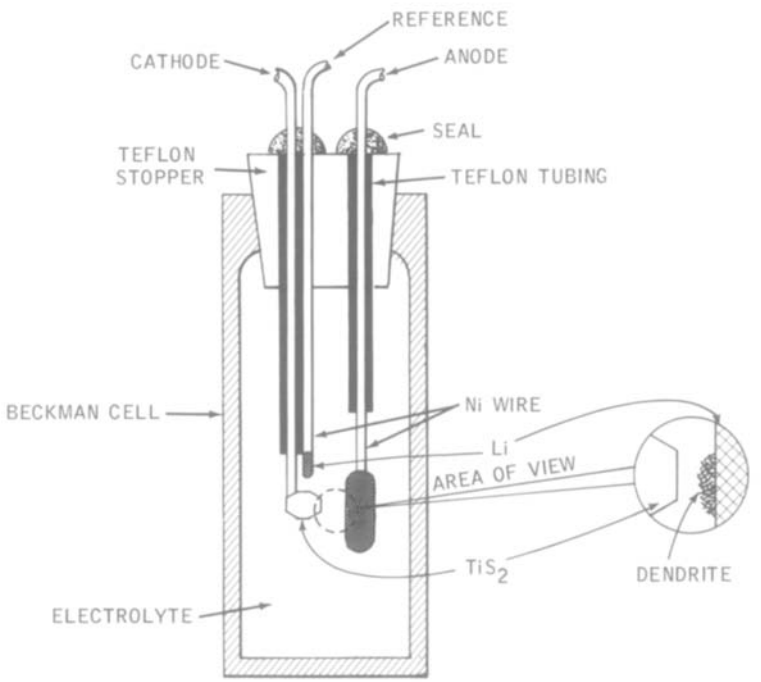

FIG. 9. Optical cell for *in situ* battery studies.

soldered to an aluminium wire with indium solder. The crystals were generally several millimeters across to facilitate ease of handling. The cell was a 1×1-cm Beckman spectrophotometer cell, and the major limitation of the technique was the working distance of the objectives used to look through the cell. A variety of objectives and methods of illumination were used with observation of various features of the processes occurring in the cell. The components were placed in the cell and the nonaqueous lithium electrolyte was added, all operations being carried out in an argon atmosphere. With the cell properly sealed, it was removed from the dry box and placed on the stage of the microscope. If the TiS_2 cathode was being observed, the position of the cell was adjusted so that the incident light was normal to the *C*-axis of the crystal. This provided the maximum reflection and the best viewing conditions. The external wire leads were attached to a PAR potentiostate/galvanostat provided with a recorder. This allowed observation of visual changes within the cell while monitoring current, voltage, and coulombs.

The cracking effect noted in large crystal was immediately confirmed in the electrochemical experiment. When a crystal was discharged at a rate of approximately 0.1 mA/cm^2 (10 μA/0.1 cm^2 edge area), the cracking continued until a lower limit of approximately 10 μm^2 was reached and proceeded no further, also in agreement with the *n*-butyllithium study. These results imply that actual working cathodes should be made of particles of less than 10 μm to avoid physical degradation due to cracking. We were unable to successfully mount crystals which were perfect enough to exhibit the boundary effect which allows precise measurements of rates of intercalation. In order to overcome this difficulty a new cell has been designed and this will be the subject of a future report. Nevertheless, the cell described above allowed the observation of several effects not

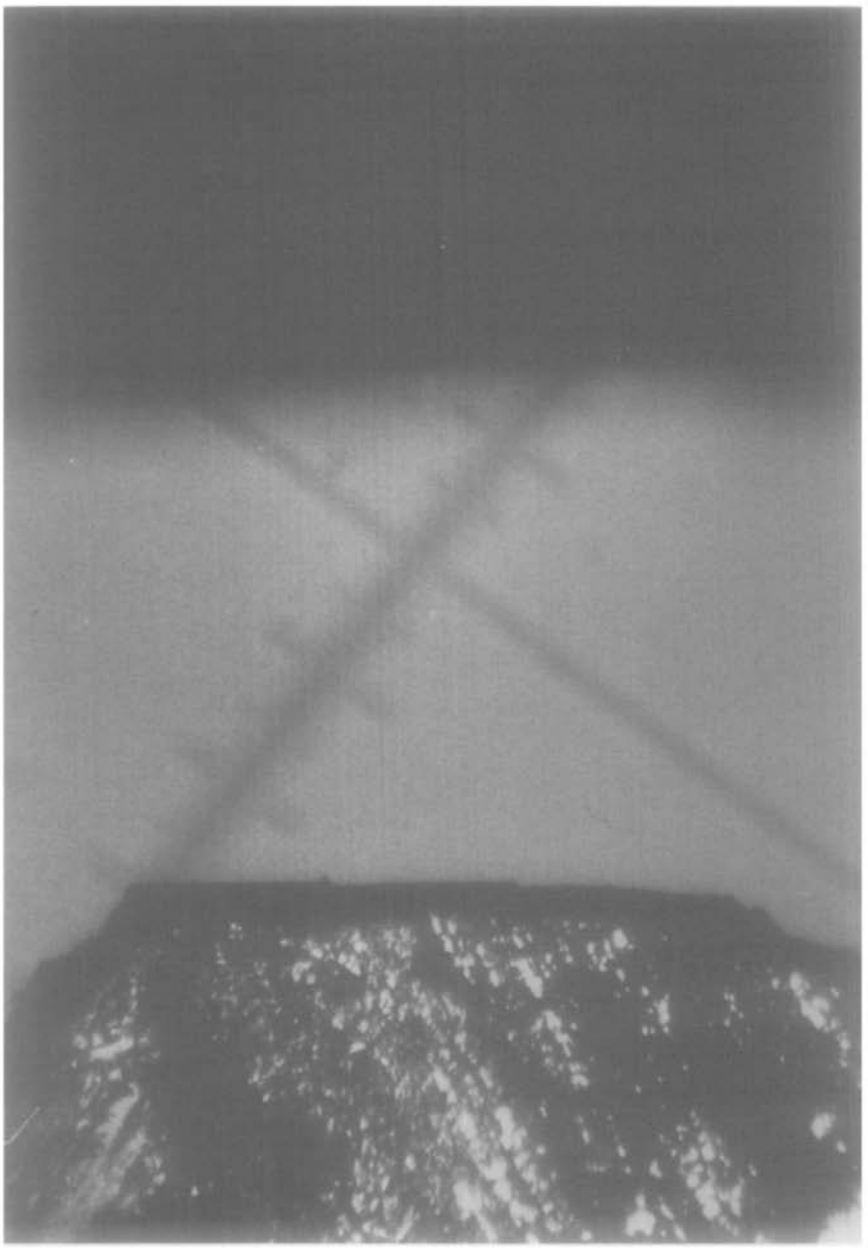

FIG. 10. Film and cracking on TiS_2 single-crystal cathode (left; anode is out of focus on right). Magnification 100×.

directly related to lithium intercalation. These effects included film formation on the cathode or anode during discharge or charge (Fig. 10), electrolyte degradation, and the formation of lithium dendrites on the anode, an example of which is given in Fig. 11.

In Situ Diffraction Techniques

In the previous sections we described optical techniques for studying the intercalation of lithium into TiS_2. In this section we describe the results of an *in situ* X-ray

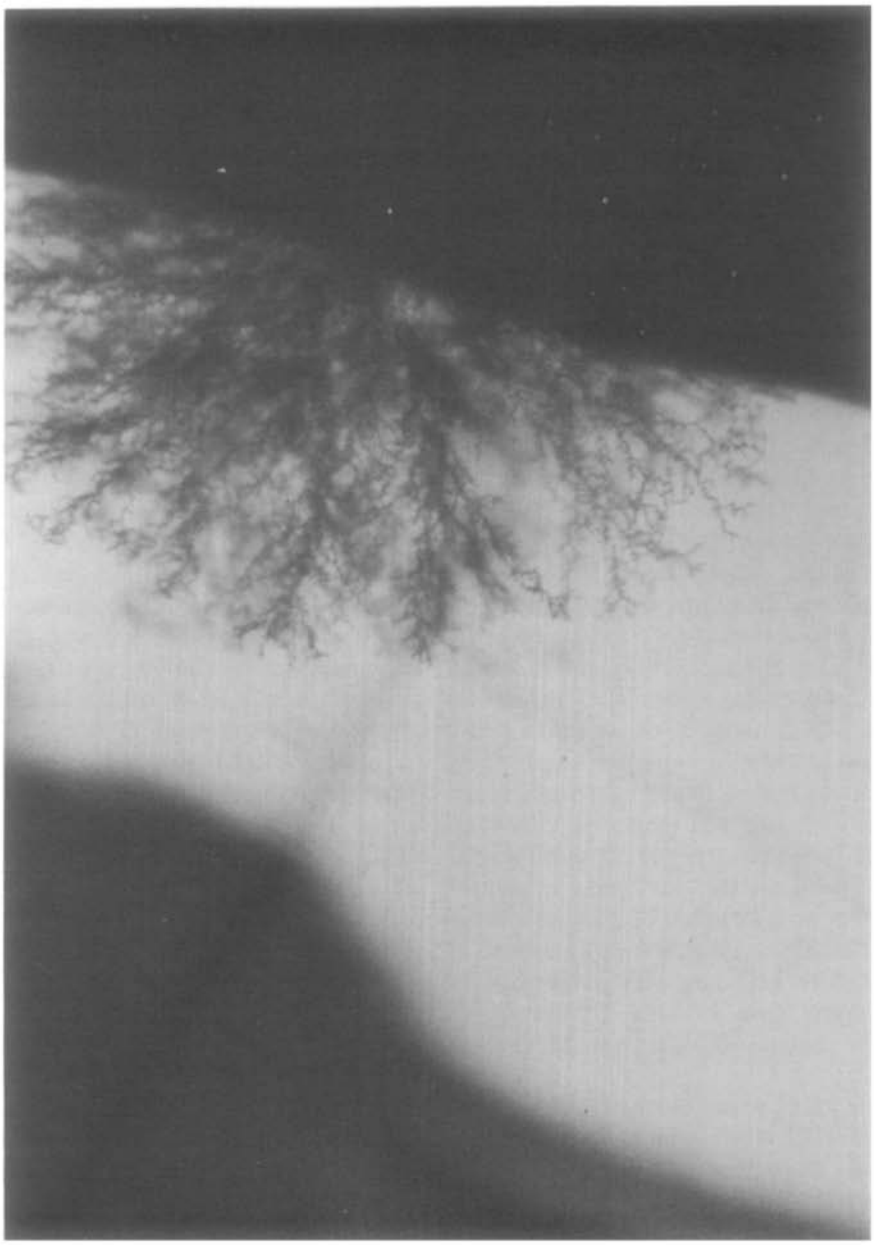

FIG. 11. Dendrite on Li anode (right; cathode is out of focus on left). Magnification 100×.

study of the same system. We have previously described the construction of an X-ray cell which allowed monitoring of structural changes at the TiS_2 cathode (or anode) during electrochemical operation (*15*). Figure 12 shows schematically the construction of the cell which allows X rays to probe the cathode through a beryllium window, while simultaneously monitoring the electrochemical potential of the cell via external leads (for details see Ref. (*15*)). The diffracted beam was received by X-ray

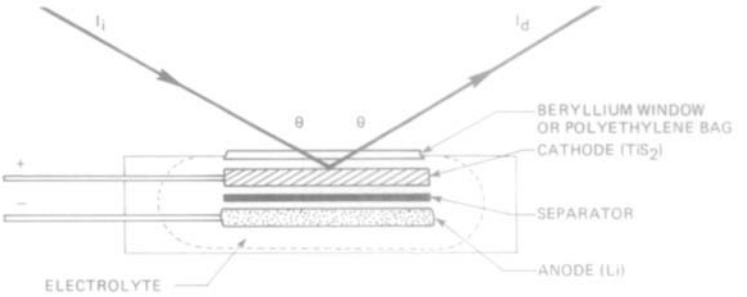

FIG. 12. Schematic of X-ray cell.

electronics and analyzed in the usual manner. For the dynamic measurement the test cell was rotated to scan continuously between predetermined Bragg angles $2\theta_1$ and $2\theta_2$, back and forth, while carrying out the electrochemical measurement. Thus the changes in the position and intensity of the peaks followed as a function of coulombs of electrochemical change identified the changes in nature and concentration of the species undergoing the electrochemical reaction. The dynamic X-ray diffraction of a TiS_2 electrode in a cathode-limiting Li/TiS_2 cell was investigated. In a typical experiment, the 100, 002, and 101 peaks of TiS_2 were scanned. These three peaks provided a convenient check on the "a" and "c" lattice parameters as a function of state of charge during the electrochemical polarization of the cell. The scanning was performed at 15 min/cycle at a rate of 1°/min in an automatic repeat sequence from 28° ($2\theta_1$) to 35° ($2\theta_2$).

The depth of penetration of Cu$K\alpha$ radiation is assessed to be ~50 μm of the 700-μm-thick TiS_2 electrode used in test cell. Thus, the changes in Bragg peak position and intensity observed during the dynamic X-ray diffraction measurements reflected the changes in the composition and crystal structure occurring in ~10% depth in thickness as measured from the position away from the lithium electrode, i.e., backside of the electrode. The X-ray spectra taken prior to switching on the electrochemical circuit served as the internal standard for the calibration of the cell.

Figure 13 represents the 101 002, and 100 Bragg peaks of a TiS_2 electrode as measured before and after discharge of a Li/TiS_2 cell at 1 mA/cm^2.

Figure 14, curve (a), illustrates the discharge data for a TiS_2 electrode of 156 m-A-hr of 4.83 cm^2 area at 1 mA/cm^2. Figure 14, curve (b), is a plot of the position of the 101 line measured during the discharge. The test electrode exhibited 90% depth of discharge with an open-circuit voltage of 1.84 V after 10 hr of rest following discharge. The position of the 101 line was determined by measuring the relative distance between the position of the 101 line on the up θ scan, and the same line on the down θ scan. This technique permitted the determination of relative line shifts with an accuracy of 0.0015 Å. Thus, each point in the curve of C-axis expansion vs χ in Li_xTiS_2, indicated by the percentage of depth of discharge in Fig. 14, consists of an average of two points which are approximately 3–4° 2θ apart.

Figure 15 gives the details of the variation of 101 peak as a function of depth of discharge. The 101 line position reflects a change in composition of the test electrode as soon as discharge began. As crystallites of Li_xTiS_2 are nucleated, their contribution to the 101 line begins, resulting in an apparent decrease in intensity and line broadening until splitting of the peaks is noticeable at ~15% depth of discharge. Only after this splitting could the previously described method for determining 101 position be used. Determination of the line position vs state of discharge at low depths of discharge

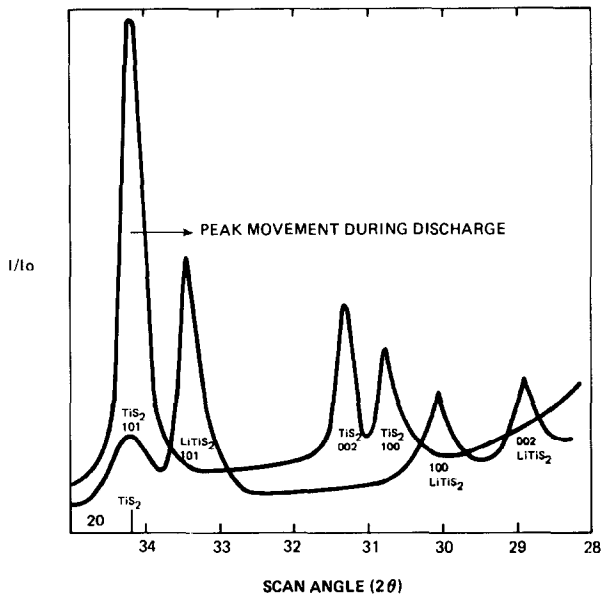

FIG. 13. Movement of Li_xTiS_2 Bragg diffraction peaks during discharge.

was possible from the continuous scan data by measuring the half-height width ($W'_{1/2} - W_{1/2}$), where $W_{1/2}$ is the height of the resolved TiS_2 or Li_xTiS peak.

One can see from Fig. 16 that up to $X = 0.3$, i.e., 30% depth of discharge, the variation in C-axis expansion is approximately linear. The point of inflection in the region of 12–18% may be attributed to lithium ordering, an effect recently reported as perhaps the pronounced plateau which begins at $\frac{1}{4}$ discharge and ends at $\frac{1}{2}$ discharge seen in Fig. 14 (*16, 17*).

Throughout the experiments, the width of the 101 line for a given χ in Li_xTiS_2 did not change, but the intensity of the peak decreased. This decrease cannot be explained by calculating the intensity of the 101 line for various compositions in Li_xTiS_2. Because of the low scattering power of

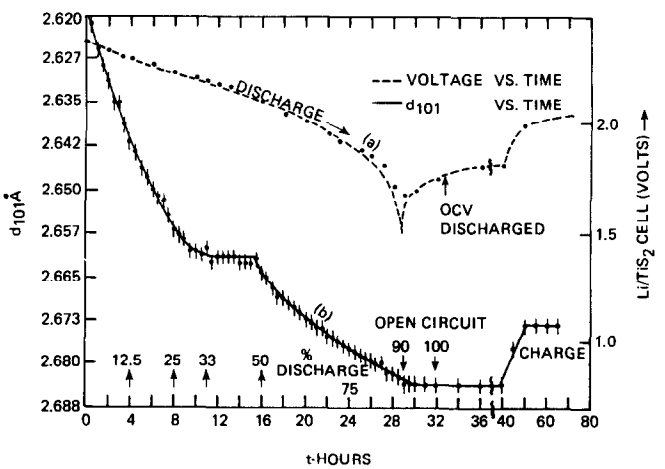

FIG. 14. Discharge for Li_xTiS_2 cell.

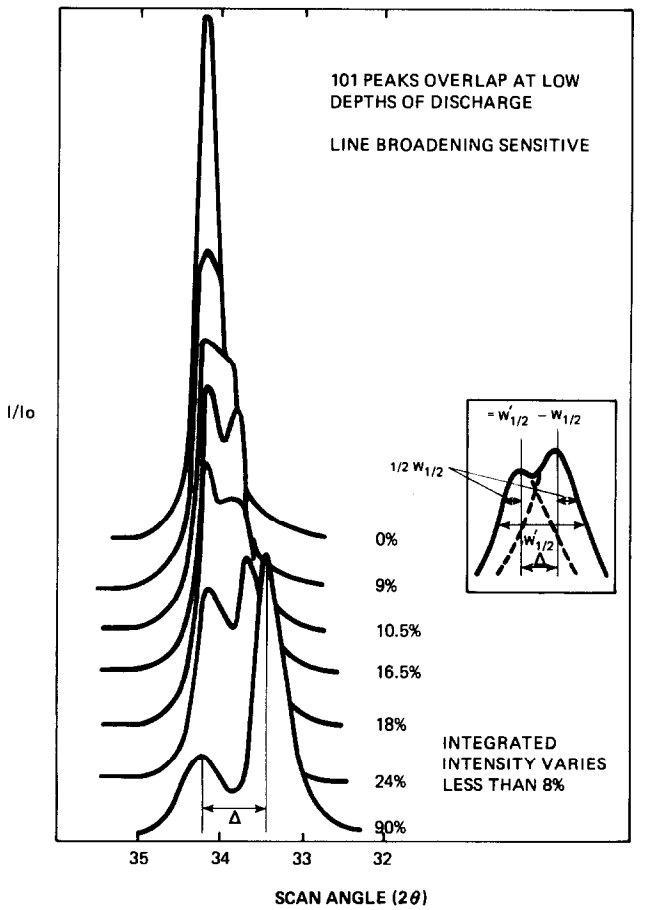

FIG. 15. Variation of Bragg peaks as a function of depth of discharge of TiS_2.

lithium atoms, no more than 10% variation is expected in the intensity of the 101 line, whereas a decrease of more than 50% is observed, as seen in Fig. 17a. Experiments indicated that upon standing on open circuit for 10 hr, this intensity is regained almost to the original value, as indicated in Fig. 17b. We propose that the observed intensity loss during the discharge is due to intercalated layers which are wrinkled or bent, and therefore do not contribute to the intensity of Bragg peaks. Upon standing on open circuit, the stressed TiS_2 layers anneal and realign themselves, causing the intensity to be regained. This is in agreement with the previously described optical studies in which the crystals are highly strained during intercalation, then relax upon completion of reaction.

Conclusions

The experiments described above allow us to draw some conclusions regarding the mechanism of intercalation of lithium into TiS_2. Hooley (*18*) has reported that if the basal planes of graphite are blocked to absorption of Br_2 it will not then intercalate. We believe that this may also be the case for the adsorption of lithium on the basal planes of TiS_2. As seen from the optical *ex situ* studies initial intercalation takes place rapidly on the thin surface layers which cover the larger TiS_2 crystals. While this does not

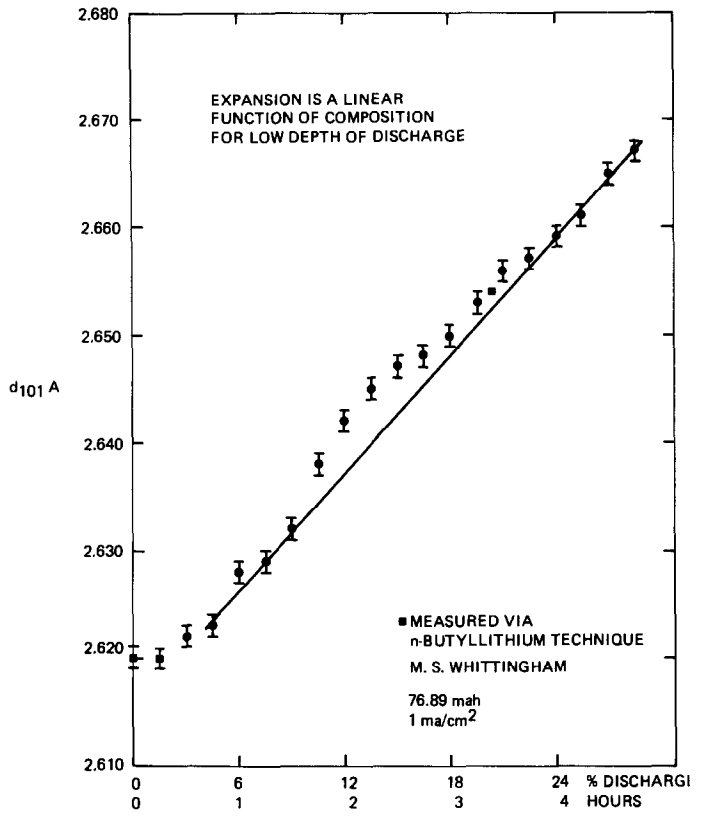

FIG. 16. Lattice expansion data for low depths of discharge.

prove that lithium must first adsorb on the basal planes of TiS_2 to allow intercalation, it does suggest this. We may also note that irreversible films which form on the basal planes during *in situ* optical studies prevented further cycling even though the crystal of TiS_2 remained intact. Further studies would be needed, however, to conclusively prove this point which has important consequences for battery rate and life capabilities.

Once the process of intercalation is initiated the crystallites undergo tremendous strain as the layers open up. If the crystals are too large or contain defects the layers crack, relieving the strain. In small crystallites the layers undergo a large distortion which itself must be governed by the bond strengths which hold the layers together. This leads to the possibility that fundamental mechanical properties of the layers could be calculated then measured by this technique. In order to do this, however, effects of crystal thickness and crystal perfection will have to be addressed. An understanding of this process would lead to an exact description of the intercalation process and the rate limiting factors which govern battery operation.

The process is further complicated by lithium ordering which causes nonuniform lattice expansion throughout the intercalation process. The *in situ* X-ray technique also demonstrates that the layers suffer great disorder. This disorder, however, is self-annealed as the X-ray intensity is regained after intercalation, in agreement with the *ex situ* optical studies. In fact, it is probably the ability of the TiS_2 layers to flex and reorder

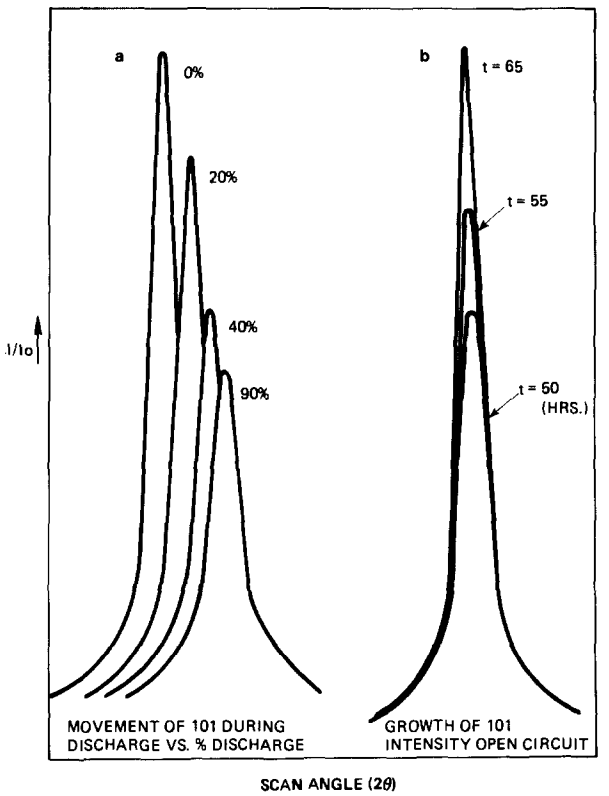

FIG. 17. Movement of 101 Bragg peaks of TiS_2 and growth of 101 peak intensity on open circuit stand.

which allows the TiS_2 to function so well as a secondary battery cathode.

The dynamic *ex situ* and *in situ* techniques described above give invaluable insight into the mechanism of lithium intercalation into TiS_2. This information is also applicable to problems which arise in cycling of batteries. Although we have concentrated on the Li/TiS_2 battery system the techniques are general and should be applicable to any battery system.

References

1. A. H. THOMPSON AND M. S. WHITTINGHAM, *Mater. Res. Bull.* **12**, 741 (1977).
2. M. S. WHITTINGHAM, *Science* **192**, 1126 (1976).
3. M. S. WHITTINGHAM, *Progr. Solid State Chem.* **12**, 41 (1978).
4. M. S. WHITTINGHAM AND R. R. CHIANELLI, "Reactivity of Solids," p. 89, Plenum, New York (1977).
5. M. S. WHITTINGHAM AND F. R. GAMBLE, *Mater. Res. Bull.* **10**, 363 (1975).
6. B. G. SILBERNAGEL AND M. S. WHITTINGHAM, *J. Chem. Phys.* **64**, 3670 (1976).
7. M. S. WHITTINGHAM, *J. Electrochem. Soc.* **123**, 315 (1976).
8. A. H. THOMPSON, F. R. GAMBLE, AND C. R. SYMON, *Mater. Res. Bull.* **10**, 915 (1975).
9. R. R. CHIANELLI, J. C. SCANLON, AND A. H. THOMPSON, *Mater. Res. Bull.* **10**, 1379 (1975); A. J. JACOBSON AND L. E. MCCANDLISH, *J. Solid State Chem.* **29**, 355 (1979).
10. M. B. DINES, *Mater. Res. Bull.* **10**, 287 (1975).
11. M. S. WHITTINGHAM, R. R. CHIANELLI, AND M. B. DINES, *in* "Electrochemical Society Meeting, Dallas, Texas, October 5–9, 1975," Paper 35.
12. R. R. CIANELLI, *J. Crystal Growth* **34**(2), 239 (1976).
13. R. R. CHIANELLI, J. C. SCANLON, AND A. H. THOMPSON, *Mater. Res. Bull.* **10**, 1379 (1975).

14. R. R. CHIANELLI, E. B. PRESTRIDGE, T. A. PECORARO, AND J. P. DENEUFVILLE, *Science*, **203**, 1105 (1979).
15. R. R. CHIANELLI, J. C. SCANLON, AND B. M. L. RAO, *J. Electrochem. Soc.* **125**, 1563 (1978).
16. A. H. THOMPSON, *Phys. Rev. Lett.* **40**, 25, 1511 (1978).
17. A. H. THOMPSON, *J. Electrochem. Soc.*, **126**, 608 (1979).
18. J. G. HOOLEY, *Chem. Phys. Carbon* **5**, 321 (1969).